Differences in Stability among the Human Apolipoprotein E Isoforms Determined by the Amino-Terminal Domain†

Julie A. Morrow,‡,§ Mark L. Segall,‖ Sissel Lund-Katz,‖ Michael C. Phillips,‖ Mark Knapp,⊥ Bernhard Rupp,⊥ and Karl H. Weisgraber*,‡,§,#

Gladstone Institute of Neurological Disease, Cardiovascular Research Institute, Department of Pathology, University of California, San Francisco, California 94110, Department of Biochemistry, MCP Hahnemann University, Philadelphia, Pennsylvania 19129, and Biology and Biotechnology Research Program, Lawrence Livermore National Laboratory, Livermore, California 94550

Received January 19, 2000; Revised Manuscript Received July 26, 2000

ABSTRACT: Denaturation by guanidine-HCl, urea, or heating was performed on the common isoforms of human apolipoprotein (apo) E (apoE2, apoE3, and apoE4) and their 22-kDa and 10-kDa fragments in order to investigate the effects of the cysteine/arginine interchanges at residues 112 and 158. Previous physical characterization of apoE3 established that apoE contains two domains, the 10-kDa carboxyl-terminal and 22-kDa amino-terminal domains, which unfold independently and exhibit large differences in stability. However, the physical properties of apoE2, apoE3, and apoE4 have not been compared before. Analysis by circular dichroism showed that the different isoforms have identical α-helical contents and guanidine-HCl denaturation confirmed that the two domains unfold independently in all three isoforms. However, guanidine-HCl, urea, and thermal denaturation showed differences in stability among the 22-kDa amino-terminal fragments of the apoE isoforms (apoE4 < apoE3 < apoE2). Furthermore, guanidine-HCl denaturation monitored by circular dichroism and fluorescence suggested the presence of a folding intermediate in apoE, most prominently in apoE4. Thus, these studies reveal that the major isoforms of apoE, which are associated with different pathological consequences, exhibit significant differences in stability.

Apolipoprotein (apo)[1] E, a 34-kDa, 299-amino acid protein (*1*), is associated with several classes of plasma and cerebral spinal fluid (CSF) lipoproteins (*2*−*5*). Through its interaction with receptors in the low density lipoprotein (LDL) receptor family (*2*, *6*−*10*), apoE transports cholesterol and triglyceride among tissues in the vasculature and nervous systems. In addition, apoE plays a role in immunoregulation (*11*−*13*) and cell growth (*14*).

Three common isoforms of apoE (apoE2, apoE3, and apoE4) are genetically determined by three corresponding alleles at a single gene locus on chromosome 19 (allelic frequency: $\epsilon 2 = 0.08$, $\epsilon 3 = 0.77$, and $\epsilon 4 = 0.15$) (*15*−*17*). The isoforms differ by cysteine and arginine content at positions 112 and 158; apoE3, the most common form, contains cysteine and arginine at these positions, respectively. Apolipoprotein E2 contains cysteine, and apoE4 arginine, at both positions (*1*, *18*).

The common isoforms of apoE have significantly different physiological and biochemical effects. ApoE4 is associated with high plasma cholesterol levels and with an increased risk for both heart disease (*19*−*21*) and Alzheimer's disease (AD) (*22*, *23*). ApoE4 is also found to be a predictor for morbidity after head injury (*24*−*26*). A subset of the population homozygous for apoE2 develop type III hyperlipidemia (*27*, *28*), and apoE2 may be protective against AD (*29*). Characterized biochemical differences between the isoforms include differential LDL receptor binding activity (*30*), association with lipoproteins (*31*−*33*), accumulation in cells (*34*, *35*), association with proteins involved in AD such as Aβ peptide (*36*−*39*) and tau (*40*−*42*), effects on neurite outgrowth (*34*, *43*−*46*), and neurotoxicity in cell culture (*47*−*50*).

Previous physical characterization of apoE3 (*51*, *52*), the most common isoform, established that it had two distinct domains (the 22-kDa amino-terminal and 10-kDa carboxyl-terminal domains) that unfold independently of each other (*51*). The 22-kDa amino-terminal domain (residues 1−191), shown by X-ray crystallographic studies to be a four-helix bundle (*53*), contains the receptor-binding region (residues in the vicinity of 136−150) (*2*, *54*−*56*). The10-kDa carboxyl-terminal domain (residues 218−299) contains important lipoprotein-binding regions (*33*, *51*, *57*−*59*). The two domains are joined by a hinge region (approximately residues 165−215) (*51*, *52*).

† This work was supported by grants from NIH Program Project Grant HL41633 and NIH Grant NS35939 and HL56083 by the United States Department of Energy at Lawrence Livermore National Laboratory under Contract W-7405-Eng-48.

* To whom correspondence should be addressed: Gladstone Institutes, P.O. Box 419100, San Francisco, CA 94141-9100. Phone: (415) 826-7500. Fax: (415) 285-5632. E-mail: kweisgraber@gladstone.ucsf.edu.

‡ Gladstone Institute of Neurological Disease.

§ Cardiovascular Research Institute.

‖ Department of Biochemistry.

⊥ Biology and Biotechnology Research Program.

Department of Pathology.

[1] Abbreviations: apo, apolipoprotein; kDa, kilodalton; LDL, low-density lipoproteins; AD, Alzheimer's disease; Aβ, amyloid peptide β; VLDL, very low-density lipoprotein; Trx, thioredoxin; IPTG, isopropyl-1-β-D-thiogalactopyranoside; DMPC, dimyristoyl phosphatidylcholine; CD, circular dichroism; DTT, dithiothreitol; β-Me, β-mercaptoethanol.

10.1021/bi000099m CCC: $19.00
Published on Web 08/26/2000

How one or two amino acid differences among the isoforms of apoE result in the differential effects listed above is a major question. Only the differential LDL receptor binding (*60*, *61*) and association of apoE isoforms with plasma lipoproteins (*58*, *62*) have been characterized at the molecular level. In apoE2, there is a rearrangement of salt bridges in helices three and four in the four-helix bundle that change the electrostatic potential in the receptor binding region (*60*) resulting in defective LDL receptor activity. In ApoE4, there is an interaction between Arg-61 in the 22-kDa amino-terminal domain and Glu-255 in the 10-kDa carboxyl-terminal domain that does not occur in apoE2 or apoE3. The apoE4 domain interaction is responsible for the preferential association of apoE4 with plasma very low-density lipoproteins (VLDL) compared to apoE3 and apoE2 preference for HDL (*58*, *62*). With the importance of apoE in lipid metabolism and the growing list of differential effects among the isoforms, it is important to determine the physical characteristics of the apoE isoforms in order to understand better their fundamental properties and potential differences as a basis for gaining insight into the differences in their metabolic behavior and role in disease.

Using guanidine-HCl, urea, and thermal denaturation, we characterized the common isoforms of apoE, and their corresponding 22-kDa (residues 1−191) and 10-kDa (residues 223−299) fragments and established that apoE2 and apoE4 also contain two independently folded domains as previously shown for apoE3 (*51*, *52*). In addition, the α-helical content of all three isoforms and their corresponding 22-kDa fragments were similar, approximately 56−64%. However, significant differences between the isoforms were also revealed by these studies. Specifically, denaturation studies monitored by circular dichroism indicated a difference in stability among the isoforms (apoE4 < apoE3 < apoE2). These studies represent the first assessment of the physical characteristics of apoE2 and apoE4 and establish differences in the thermodynamic properties among the common isoforms of human apoE. These findings may provide insight into known differential association of apoE isoforms with risk for heart disease and neurodegeneration, including Alzheimer's disease.

MATERIALS AND METHODS

Expression and Purification of ApoE and Fragments of ApoE. Purification of full-length apoE was carried out as described previously (*63*). The 22-kDa and 10-kDa (*64*) fragments of apoE were purified according to the same protocol with some modifications. Briefly, the cDNA for full-length human apoE2, apoE3, apoE4, the 22-kDa fragments of each isoform (residues 1−191), or the 10-kDa fragment of human apoE (residues 223−299) was ligated into a thioredoxin (Trx) fusion expression vector (pET32a, Novagen) and transformed into the *Escherichia coli* strain BL21 (DE3) (Novagen) (*63*, *64*).

The transformed *E. coli* were cultured in LB medium at 37 °C, and Trx-apoE expression was induced with IPTG (final concentration, 100 μg/mL) for 2 h. After the bacterial pellet was sonicated and the lysate was centrifuged to remove debris, the Trx fusion protein, which contains a His-tag, was purified on a nickel affinity column. The fusion protein was then cleaved with thrombin to remove Trx from apoE, the 22-kDa, or 10-kDa fragment.

For purification of full-length apoE, the fusion protein was complexed with dimyristoyl phosphatidylcholine (DMPC) before it was cleaved with thrombin to protect the protease susceptible hinge region. After inactivation of the thrombin with β-mercaptoethanol (β-Me), the mixture was lyophilized, delipidated, and the protein was solubilized in 6 M guanidine-HCl (in 0.1 M Tris, pH 7.4, 0.01% EDTA, and 1% β-Me). Protein was isolated by gel filtration chromatography on Sephacryl S-300 in 4 M guanidine-HCl (in 0.1 M Tris, pH 7.4, 0.01% EDTA, and 0.1% β-Me). The fractions containing apoE were pooled, dialyzed against 5 mM NH_4HCO_3, and lyophilized. The protein was solubilized in 100 mM NH_4HCO_3 and stored at −20 °C.

For purification of the 22-kDa and 10-kDa fragments, association of the fusion proteins with DMPC prior to thrombin cleavage was not necessary. After cleavage was complete and the thrombin was inactivated with β-Me, the mixture was repassed on a nickel affinity column to remove Trx. The 22-kDa or 10-kDa fragment was then dialyzed into 6 M guanidine-HCl (in 0.1 M Tris, pH 7.4, 0.01% EDTA, and 1% β-Me). Protein was isolated by filtration chromatography as described above.

Guanidine Denaturation. ApoE and the 22- and 10-kDa fragments were analyzed by guanidine-HCl denaturation. Protein (500 and 100 μg/mL) was incubated overnight at 4 °C in 20 mM sodium phosphate, pH 7.4, 1 mM dithiothreitol (DTT), and guanidine-HCl at various concentrations. Circular dichroism (CD) measurements were made on a Jasco 715 spectropolarimeter at 25 °C. All experiments were performed under reducing conditions. Molar ellipticity ([θ]) at 220 nm was calculated from the relationship

$$[\theta] = (\mathrm{MRW})(\theta_{220})/10lc \qquad (1)$$

where θ_{220} is the measured ellipticity at 220 nm in degrees, l is the cuvette path length (0.1 cm), and c is the protein concentration (g/mL). A mean residue weight (MRW) of 114 was used.

$\Delta G°$ was calculated by using nonlinear regression (Prism, Graphpad) to fit the data showing the dependence of θ on the concentration of guanidine-HCl to the following sigmoidal equation (*65*):

$$-RT \ln K_D = \Delta G° - \Delta nRT \ln(1 + ka) \qquad (2)$$

where $\Delta G°$ is the free energy of denaturation at 0 M guanidine-HCl, Δn is the difference in the number of moles of guanidine-HCl bound in the denatured and native states, R is the gas constant, T is temperature, k is the association constant for guanidine-HCl, and a is the molarity of guanidine-HCl. The equilibrium constant for the denaturation reaction (K_D) is determined by the formula

$$K_D = (\theta_N - \theta)/(\theta - \theta_D) \qquad (3)$$

θ_N is the molar ellipticity of the protein in its native conformation, θ_D is the molar ellipticity when it is denatured, and θ is the ellipticity at a given concentration of guanidine-HCl. The variables used in fitting to eq 2 were $\Delta G°$ and Δn. θ_N and θ_D were taken as constants because, as discussed before (*66*), extrapolation of the initial and final slopes of apolipoprotein denaturation curves leads to unacceptable interassay variability. $\Delta G°$ values in the absence of denatur-

ant were also calculated by plotting $\Delta G°$ against guanidine-HCl concentration and extrapolating to zero concentration (*67*). Comparison of slopes, *m*, of the linear regression lines for protein mutants gives insights into likely structural changes due to point mutations (*68*).

Urea Denaturation. The 22-kDa fragments of apoE were analyzed by urea denaturation. Protein (100 μg/mL) was incubated overnight at 4 °C in 20 mM sodium phosphate, pH 7.4, 0.15 M NaCl, 1 mM DTT, and freshly deionized urea at various concentrations. CD measurements and calculations were performed as described above.

Fluorescence Measurements. Guanidine-HCl denaturation of the 22-kDa fragments of apoE3 and apoE4 was monitored by tryptophan fluorescence. Protein (100 μg/mL) was incubated overnight at 4 °C in 20 mM sodium phosphate, pH 7.4, 1 mM DTT, and guanidine-HCl at various concentrations. Measurements were made on an Hitachi F2000 fluorimeter at 25 °C using an excitation wavelength of 295 nm and monitoring an emission scan from 285 to 400 nm. The average emission wavelength was calculated as the intensity weighted average of the emission wavelengths.

Thermal Denaturation. ApoE and the 22- and 10-kDa fragments were analyzed by thermal denaturation. Thermal scans were conducted on protein (50 μg/mL in 10 mM sodium phosphate buffer, pH 7.4, freshly dialyzed from 1% β-mercaptoethanol and 6 M guanidine-HCl solution) at a rate of 1 °C/min from 20 °C to 90 °C. Control experiments using SDS−PAGE analysis showed that there was insignificant oxidation and disulfide bond formation in apoE2 and apoE3 samples after denaturation. Measurements were done in triplicate for each sample using a Neslab RTE−111 circulation water bath to heat the sample which was in a jacketed quartz cuvette. Temperature (*T*)-induced unfolding was monitored by electronic recording of the CD change (using a Jasco J-600 spectropolarimeter) at 222 nm. Data showing the fractional change in $[\theta]_{222}$ as a function of temperature were fitted by nonlinear regression using the Boltzmann sigmoidal equation (Prism, Graphpad). As described previously (*66*), the α-helix contents were calculated from the molar ellipticity values derived from eq 1, although these measurements were done at 222 nm. The α-helix content of each protein sample was computed using eq 4

$$\% \text{ α-helix} = (-[\theta_{222}] + 3000)/39000 \qquad (4)$$

Thrombin Cleavage of Full-length ApoE4. Thrombin (Haematologic Technologies, Inc.) was added to full-length apoE4 (0.5 mg/mL, PBS, pH 7.4) at a ratio of 850:1 (apoE: thrombin, w/w) and incubated at 37 °C. At various time points 200 μL aliquots were analyzed by gel filtration chromatography (TSK 3000_{XL} SW column, 0.5 mL/min, PBS, pH 7.0). Purified apoE4 and its corresponding 22-kDa and 10-kDa fragments were used as size standards.

RESULTS

Assessment of Helical Content of the 22-kDa Fragments and Full-Length Human ApoE Isoforms. The secondary structural content of recombinant apoE isoforms and their corresponding 22-kDa fragments (residues 1−191) was examined by circular dichrosim (CD). The α-helical contents of all three isoforms and their 22-kDa amino-terminal fragments were calculated from their molar ellipticities at 222 nm ($\theta_{222} = -19\,000 - -22\,000$) using eq 4 and ranged from 56 to 64%. Taking into account an approximate error of 5% in the measurements, there appeared to be no significant difference in the α-helical content between the isoforms, and the θ_{222} measurements of apoE3 and its 22-kDa fragment were similar to those in previously published reports (*52*, *69*).

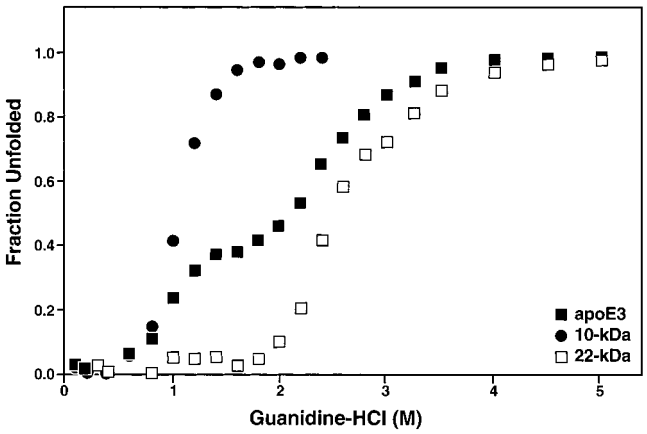

FIGURE 1: Guanidine-HCl denaturation of apoE3 and its 22-kDa and 10-kDa fragments. The molar ellipticity of protein was measured at 220 nm at a concentration of 0.5 mg/mL in 20 mM sodium phosphate, pH 7.4, 1 mM dithiothreitol, and various concentrations of guanidine-HCl. Fraction Unfolded was calculated using eq 6.

Chemical Denaturation of the 22-kDa Fragments, 10-kDa Fragment, and Full-Length Human ApoE Isoforms. The structural stabilities of recombinant human apoE isoforms (apoE2, apoE3, and apoE4, the 22-kDa fragments of each isoform, and 10-kDa fragment) were examined by guanidine-HCl denaturation. It was established previously that recombinant apoE3 displayed an identical guanidine denaturation curve to that of apoE3 isolated from plasma (*63*). The concentration of guanidine-HCl at which half-maximal denaturation ($D_{1/2}$) occurred was obtained by fitting data points to the optimal variable-slope sigmoidal curve

$$Y = \theta_D + (\theta_N - \theta_D)/(1 + 10^{[(D_{1/2}-X)h]}) \qquad (5)$$

by nonlinear regression. *Y* is the ellipticity at a given guanidine-HCl concentration, *X* is the molar concentration of guanidine-HCl, and *h* is the Hill coefficient (slope) (*70*). θ_N is the molar ellipticity of protein sample in its native conformation, and θ_D is the molar ellipticity when it is denatured. Figure 1 shows the relationship between guanidine-HCl concentration and fraction unfolded of apoE3 and its corresponding 22-kDa and 10-kDa fragments. The fraction of the protein unfolded is defined as

$$\text{Fraction Unfolded} = (\theta)_N - (\theta)/(\theta)_N - (\theta)_D \qquad (6)$$

where θ_n and θ_d are defined above, and θ is the ellipticity at a given guanidine-HCl concentration.

The denaturation curve of apoE3 was biphasic. For $D_{1/2}$ calculations, we assumed that each phase of the biphasic denaturation could be treated as an individual two-state denaturation equilibrium. The first phase of the denaturation curve for apoE3 had a calculated $D_{1/2}$ of 0.95 ± 0.05 M guanidine-HCl, and the second phase, 2.44 ± 0.03 M guanidine-HCl. The 10-kDa and 22-kDa fragments each

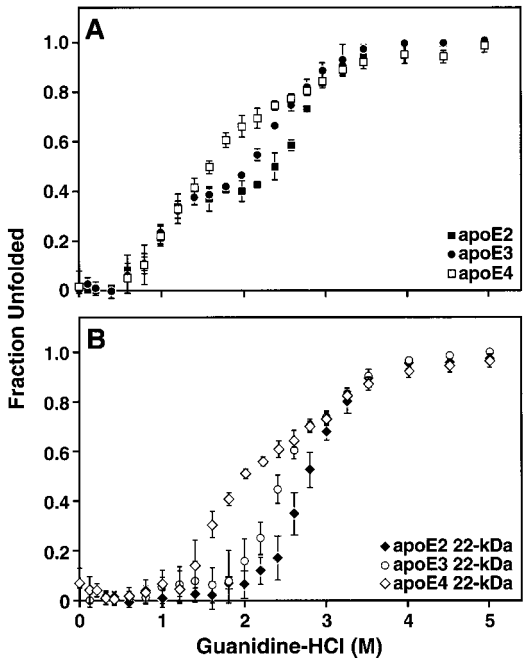

FIGURE 2: Guanidine-HCl denaturation of apoE2, apoE3, apoE4 (A), and their corresponding 22-kDa fragments (B). The molar ellipticity of protein was measured at 220 nm at a concentration of 0.5 mg/mL in 20 mM sodium phosphate, pH 7.4, 1 mM dithiothreitol, and various concentrations of guanidine-HCl. Fraction Unfolded was calculated using eq 6. Each denaturation was done at least three times on different preparations of protein. The bars represent the standard deviation.

showed a denaturation profile that fit a typical two-state denaturation equilibrium. The $D_{1/2}$ for the 10-kDa and 22-kDa fragment denaturation curves were 1.05 ± 0.02 and 2.51 ± 0.04 M guanidine-HCl, respectively. Thus, the first phase of the denaturation curve of apoE3 corresponded to the 10-kDa fragment and the second phase to the 22-kDa fragment. These results are consistent with those published by Wetterau et al. (*51*) on apoE3 purified from plasma and its thrombolytic fragments.

We next examined the guanidine-HC1 denaturation for all three isoforms and their corresponding 22-kDa fragments (Figure 2). The denaturation curve for apoE2 was biphasic, and the plateau between the first and second phases occurred at approximately 1.6 M guanidine-HCl, similar to that of apoE3. The calculated midpoints of denaturation for the first and second phases of the denaturation curve for full-length apoE2 were 0.95 ± 0.02 and 2.66 ± 0.04 M guanidine-HCl, respectively. The denaturation curve for the 22-kDa fragment of apoE2 fit a two-state equilibrium and had a $D_{1/2}$ of 2.78 ± 0.05 M guanidine-HCl. Thus, as with apoE3, the first and second phases of the denaturation curve for full-length apoE2 correspond to its 10-kDa carboxyl-terminal and 22-kDa amino-terminal domains, respectively. This suggests that the two domains in apoE2 also unfold independently of each other. The differences in $D_{1/2}$ between the 22-kDa fragments of apoE2 and apoE3 were statistically significant ($p < 0.001$), with apoE2 having a higher $D_{1/2}$ than apoE3. The $D_{1/2}$ values above are for 0.5 mg/mL solutions of apoE. Similar values were obtained when the protein concentration was reduced to 0.1 mg/mL (Figure 4A).

The denauration curve of full-length apoE4 was also biphasic but very different from that of apoE2 and apoE3.

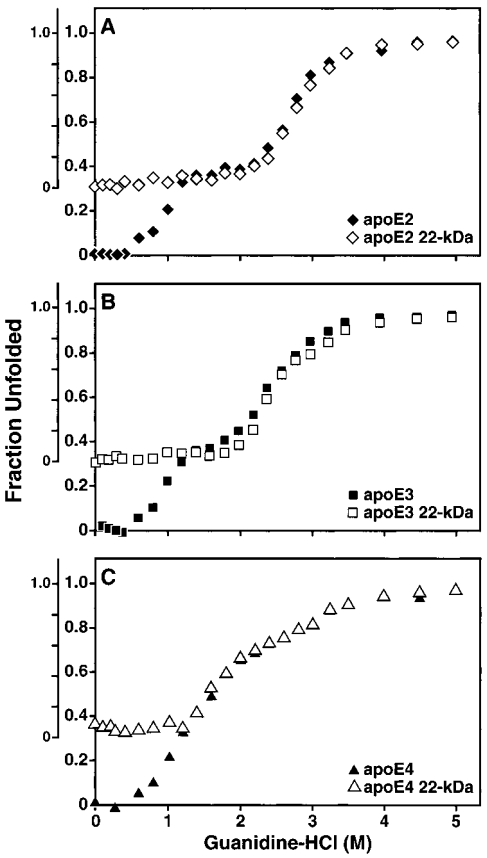

FIGURE 3: Direct comparison of guanidine-HCl denaturation curves of the full-length apoE isoforms and their 22-kDa fragments. The molar ellipticity was measured at 220 nm at a concentration of 0.5 mg/mL in 20 mM sodium phosphate, pH 7.4, 1 mM dithiothreitol, and various concentrations of guanidine-HCl. Fraction Unfolded was calculated using eq 6. All denaturation studies were done at equal concentrations of protein. Since the 22-kDa fragment represents approximately two-thirds of the full-length protein, the denaturation curve for the 22-kDa fragments were scaled down by one-third and plotted with the denaturation curve of the corresponding full-length isoform.

Specifically, the curve for full-length apoE4 displayed a slight shoulder, at approximately 2.5 M guanidine-HCl. (Figure 2A) The denaturation curve of the 22-kDa fragment of apoE4, also biphasic, contained a shoulder at 2.5 M guanidine-HCl (Figure 2B), similar to that seen in the curve for full-length apoE4. Thus, the second phase of the denaturation curve of the 22-kDa fragment of apoE4 corresponds to the second phase of the curve for the full-length protein. This implies that in the first phase of the denaturation curve for full-length apoE4, the 10-kDa fragment is not distinct from the first phase of the 22-kDa fragment. This is likely due to the smaller difference in the midpoint of denaturation between them ($\Delta D_{1/2} = 0.6$ M guanidine-HCl) compared to that difference between the 10-kDa fragment and the 22-kDa fragments of apoE2 or apoE3 ($\Delta D_{1/2} = 1.4-1.8$ M guanidine-HCl). It is also possible that the first phase of the guanidine-HCl denaturation curve for full-length apoE4, which includes both the 10-kDa domain and the first phase of the 22-kDa domain, is indicative of apoE4 domain interaction.

To confirm that in the unfolding of the full-length protein the 22-kDa domains were not affected by the 10-kDa domain, we directly compared the denaturation curve of each full-length isoform with the curve for its corresponding 22-kDa

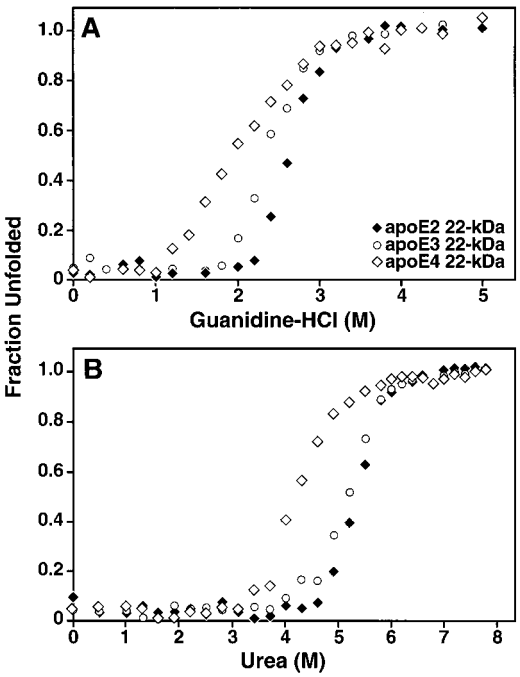

FIGURE 4: Guanidine-HCl (A) and urea (B) denaturation of the 22-kDa fragments of apoE. (A) The molar ellipticity was measured at measured at 220 nm at a concentration of 0.1 mg/mL in 20 mM sodium phosphate, pH 7.4, 1 mM dithiothreitol, and various concentrations of guanidine-HCl. (B) The molar ellipticity was measured at measured at 220 nm at a concentration of 0.1 mg/mL in 20 mM sodium phosphate, pH 7.4, 0.15 M NaCl, 1 mM dithiothreitol, and various concentrations of freshly deionized urea. Fraction Unfolded was calculated using eq 6.

fragment. Equal concentrations of protein were used in all the guanidine-HCl denaturation experiments described above. Since the 22-kDa fragment represents approximately two-thirds of the mass of the full-length protein, the curves for the 22-kDa fragments were scaled down by one-third and compared to the curves for the full-length apoE (Figure 3). The curves for the 22-kDa fragments superimpose exactly to the latter part of the curve for the corresponding full-length protein. In addition, when the guanidine-HCl curve for a 22-kDa fragment was added to the guanidine-HCl curve for the 10-kDa fragment, it was identical to the curve for the corresponding full-length isoform (data not shown). Thus, the unique character of the denaturation curve for full-length apoE4 is not due to domain interaction, and the physical properties of the 22-kDa amino-terminal domains can be assessed independently of the 10-kDa carboxyl-terminal domain. The $D_{1/2}$ of the 22-kDa fragments of apoE2, apoE3, and the first phase of the 22-kDa fragment of apoE4 were statistically different from each other ($D_{1/2} = 2.78 \pm 0.05$, 2.51 ± 0.04 and 1.60 ± 0.05 M guanidine-HCl, respectively) ($p < 0.05$). The $D_{1/2}$ of the second phase of the 22-kDa fragment of apoE4 was identical to that of the 22-kDa fragment of apoE2.

Figure 4A shows guanidine-HCl denaturation curves of the 22-kDa fragments of apoE examined at a protein concentration of 0.1 mg/mL. The shoulder in the curve for the guanidine-HCl denaturation of the 22-kDa fragment of apoE4 was present but less pronounced under these conditions, indicating a dependence on protein concentration. However, these curves show that the unfolding of the 22-kDa fragment of apoE4 is much less cooperative than for

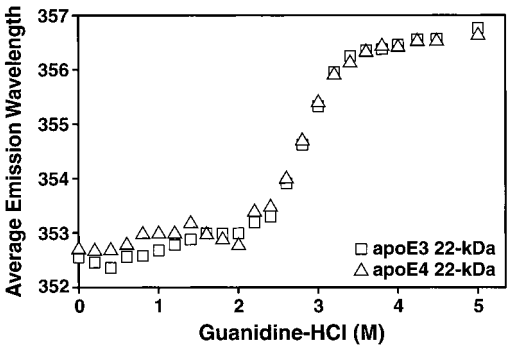

FIGURE 5: Guanidine-HCl denaturation of the 22-kDa fragments of apoE3 and apoE4 as monitored by fluorescence. Protein was studied at a concentration of 0.1 mg/mL in 20 mM sodium phosphate, pH 7.4, 1 mM dithiothreitol, and various concentrations of guanidine-HCl. Denaturation was examined using an excitation wavelength of 295 nm and monitoring an emission scan from 285 to 400 nm. The average emission wavelength is the intensity weighted average of the emission scan.

apoE3 or apoE2. Therefore, the unique behavior of apoE4 in these experiments is likely due to the intramolecular behavior of the monomer as well as a contribution from intermolecular interaction. The $D_{1/2}$ values calculated for the 22-kDa fragments of apoE2, apoE3, and apoE4 from these curves were 2.6, 2.4, and 2.0 M guanidine-HCl, respectively.

The guanidine-HCl denaturation for all the apoE isoforms and fragments was reversible. Specifically, samples diluted from a high concentration of guanidine-HCl had the expected molar ellipticity as samples originally prepared at a lower guanidine-HCl concentrations. The expected molar ellipiticity after dilution was attained in less than 45 s for all three isoforms.

To compare the effects of guanidine-HCl denaturation of the 22-kDa fragments of apoE on α-helix content and tryptophan exposure, denaturation was also monitored by fluorescence. Figure 5 shows the change in average emission wavelength of the 22-kDa fragments of apoE3 and apoE4. The curves are similar between the isoforms ($D_{1/2} = 2.8$ M guanidine-HCl) but they are different from the respective guanidine-HCl denaturation curves monitored by CD (Figure 4A). This suggests the presence of a folding intermediate or intermediates in apoE (*71*).

To eliminate a possible salt effect of guanidine-HCl and to confirm that the differences among the isoforms were not due to measurements performed in low ionic strength buffer, we examined urea denaturation of the 22-kDa fragments of apoE in a phosphate buffer containing physiologic concentrations of salt (0.15 M NaCl). Urea denaturation of the 22-kDa fragments showed the same order of denaturation midpoints (apoE4 < apoE3 < apoE2). The $D_{1/2}$ values derived from the denaturation curves shown in Figure 4B give values of 5.4, 5.2, and 4.2 M urea for the 22-kDa fragments of apoE2, apoE3 and apoE4, respectively.

Thermal Denaturation of the 22-kDa Fragments, 10-kDa Fragment, and Full-Length Human ApoE Isoforms. The isoforms of apoE were also analyzed by thermal denaturation. The percent change in molar ellipticity of apoE was plotted against temperature for the full-length isoforms and the 22-kDa and 10-kDa fragments (Figure 6). The temperatures at which there was a 50% change in the helical content of the protein (T_m) for apoE4, apoE3, and apoE2 were 45, 46, and 52 °C, respectively. While there was a trend (apoE4 < apoE3

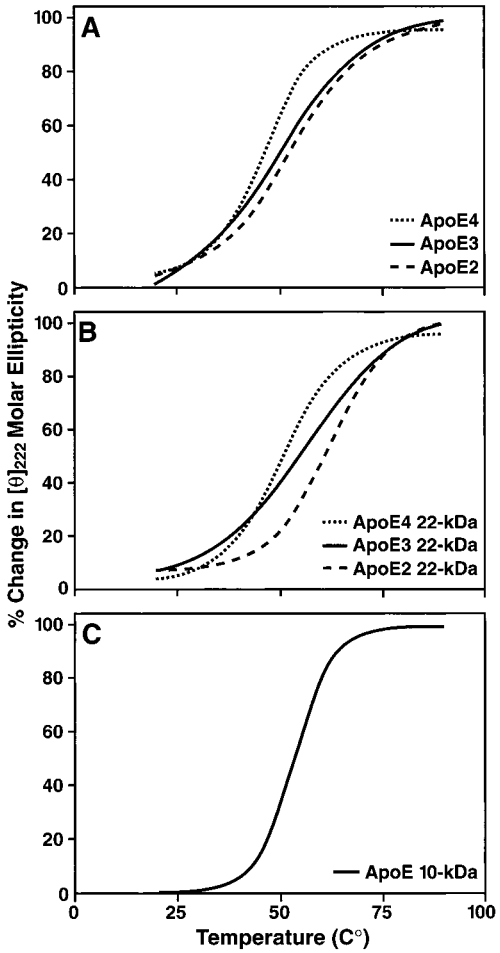

FIGURE 6: Thermal denaturation of apoE2, apoE3, apoE4 (A), and their corresponding 22-kDa fragments (B), and 10-kDa fragment (C). Thermal scans were conducted on protein (50 μg/mL in 10 mM sodium phosphate buffer, pH 7.4, freshly dialyzed from 1% β-mercaptoethanol and 6 M guanidine-HCl solution) at a rate of 1 °C/min from 20 to 90 °C. The molar ellipticity of protein was measured at 222 nm using eq 1. Each curve represents the best fit from the average of at least three scans.

< apoE2), only the T_m for apoE2 was significantly different ($p < 0.001$). However, the T_m for the 22-kDa fragments of apoE4, apoE3, and apoE2 (50, 57, and 63 °C, respectively) were statistically significant from each other ($p < 0.001$). The 10-kDa fragment had a T_m of 56 °C and its contribution is likely the reason for the lack of statistical significance between the full-length isoforms. Thus, the thermal denaturation studies confirmed a difference among the 22-kDa domains of the apoE isoforms and displayed the same order of denaturation midpoints (apoE4 < apoE3 < apoE2).

Thrombin Cleavage of Full-Length ApoE4. Although apoE4 domain interaction was not apparent in the guanidine-HCl denaturation experiments, we examined whether we could detect domain interaction in solution without denaturants. Specifically, we assessed the association of the thrombin cleavage products of apoE4 as had been done previously with apoE3 (*52*). In solution, apoE is a stable tetramer (*69*) and the tetramerization domain resides in the carboxyl-terminal fragment (*52*, *57*). Previous studies showed that when apoE3 was cleaved with thrombin, the 10-kDa fragment eluted as a tetramer and the 22-kDa fragment as a monomer on a gel filtration column and thus, the two domains did not remain associated. This contributed to the proposal that apoE3 had two independent domains (*52*). We examined apoE4 in a similar manner (described in the Materials and Methods). Analysis by gel filtration chromatography of thrombin digested apoE4 shows the release of the 22-kDa fragment and a tetramer of the 10-kDa fragment (Figure 7). Therefore, the two domains did not remain associated. Thus, apoE4 domain interaction is limited to a lipid surface where it was initially characterized (*58*, *62*).

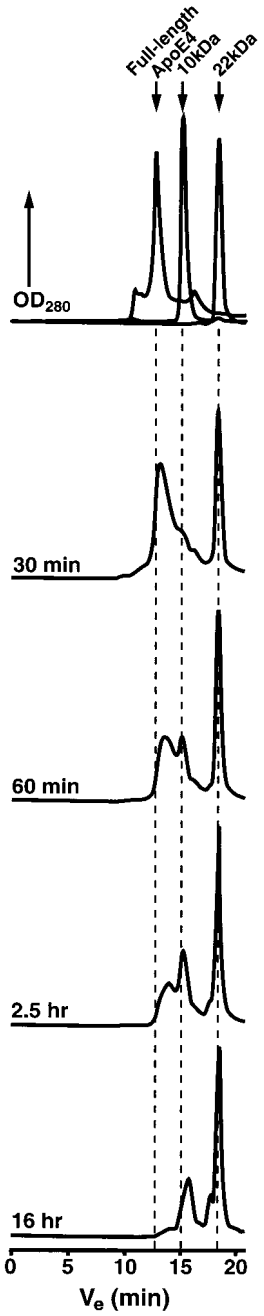

FIGURE 7: Gel filtration chromatography of the thrombin-catalyzed hydrolysis of human apoE4. Thrombin was added to apoE4 at a ratio of 850:1 (apoE:thrombin, w/w) and incubated at 37 °C. At the indicated time intervals after the beginning of hydrolysis, 200 μL of the reaction mixture (100 μg of apoE) was injected onto a TSK 3000_{XL} SW column (0.5 mL/min, PBS, pH 7.0). The elution positions of full-length apoE, the 22-kDa fragment and the tetramer of the 10-kDa fragment are indicated.

DISCUSSION

Because of the isoform-specific effects in various diseases, it is important to understand the basic physical chemical

properties of the apoE isoforms. Ultimately, the physical properties of apoE will influence its functions (i.e., how it associates with lipid and other proteins and how the cell metabolizes it). The common isoforms of apoE and their 22-kDa and 10-kDa fragments were examined by guanidine-HCl, urea, or thermal denaturation. These studies represent the first assessment of the physical characteristics of apoE2 and apoE4.

Previous physical characterizations of apoE3 revealed its unique nature compared to other apolipoproteins (*51*, *52*). Specifically, apoE3 was found to have two domains that unfold independently of each other and do not interact over a wide range of protein concentrations. Furthermore, the behavior of the 22-kDa amino-terminal domain was more similar to other globular proteins than to other apolipoproteins (*51*). The guanidine-HCl denaturation curves presented here for recombinant apoE3 and its 22-kDa amino-terminal and 10-kDa carboxyl-terminal fragments (Figure 1) were identical to those previously published by Wetterau et al. (*51*) on apoE3 purified from plasma. Here we report characterization of the 10-kDa fragment by thermal denaturation and the T_m was approximately 56 °C (Figure 6C). The analysis of the guanidine-HCl and thermal denaturation curves show that the 10-kDa fragment is similar to other apolipoproteins examined thus far (apoA-I, apoA-II, apoA-IV, apoC−I, and apoC−II) which have low midpoints of guanidine-HCl denaturation (0.4−1.1 M guanidine-HCl) (*66*, *72*−*76*) and relatively high T_m values ranging from 50 to 57 °C (*66*, *76*−*78*).

In addition, we established that the secondary structure content was approximately the same among all three isoforms and that the 22-kDa and 10-kDa domains unfold independently of each other in apoE2 and apoE4 as well as apoE3 (Figures 2 and 3). For the full-length isoforms, the guanidine-HCl denaturation curves differed from each other only in the latter part of the curve that corresponds to the 22-kDa amino-terminal domain (Figure 2A). This difference was also seen in the guanidine-HCl denaturation curves for the 22-kDa fragments alone (Figure 2B and 4A), and the midpoints of denaturation for the 22-kDa fragments were statistically different among all the isoforms (apoE4 < apoE3 < apoE2). The midpoints for urea (Figure 4B) and thermal (Figure 6B) denaturation of the 22-kDa fragments of apoE paralleled those of the guanidine-HCl denaturation (apoE4 < apoE3 < apoE2).

The apparent $\Delta G°$ values calculated for the 22-kDa fragments of apoE2, apoE3, and apoE4 (Figure 4A) using eq 2 were 8.5, 6.6, and 3.4 kcal/mol, respectively. The Δn values determined from the analysis were 25, 21, and 12 mol of guanidine-HCl, respectively. Analysis using the linear extrapolation procedure (*67*) gave consistent $\Delta G°$ values. The urea denaturation data in Figure 4B gave apparent $\Delta G°$ values of 11.3, 7.7, and 5.2 kcal/mol for the 22-kDa fragments of apoE2, apoE3, and apoE4, respectively. These values reaffirm the order of stability predicted by the $D_{1/2}$ values. Differences in $\Delta G°$ values between experiments can be attributed to differences in ionic strength of the buffer. Comparison of the *m* values derived from the slopes of the linear extrapolations for guanidine-HCl and urea denaturation (Figure 4) indicates that, relative to the wild-type apoE3 molecule, apoE2 is a m^+ mutant and apoE4 is an m^- mutant (*68*). The difficulty in interpreting the effects of point mutations on $\Delta G°$ values is in knowing whether to ascribe the change to alterations in the native state or in the denatured state. Shortle (*68*) has proposed that variations in the structure of the denatured molecule can be important. On this basis, an m^+ mutant such as apoE2 is most likely due to the arginine to cysteine substitution at residue 158 causing this isoform to unfold more completely than the parent apoE3 molecule. The mechanism responsible for m^- mutants is more ambiguous.

Since the progressive replacement of cysteine (volume = 86 Å^3) by arginine (volume = 158 Å^3) residues on changing from apoE2 to apoE4 introduces relatively bulky and charged side chains into the four-helix bundle structure, alterations in the native structure can be anticipated, although gross disruptions are not discernible at the current resolution of the X-ray structures. The cysteine to arginine substitution at residue 112 seems to be more destabilizing because the difference in stability between apoE3 and apoE4 is greater than that between apoE3 and apoE2. This mutation also seems to create domains of differing stability in the apoE4 four-helix bundle structure. The latter effect may involve some apoE4 intermolecular interactions because the non-two-state denaturation is more pronounced at higher protein concentrations. Also, the existence of unfolding intermediates is more apparent when guanidine-HCl rather than urea is used as the denaturant. This presumably reflects the differences in guanidine and urea binding to apoE4. Structural characterization of the intermediate is needed to understand this effect.

Recent analysis of different crystal forms of the amino-terminal fragment of apoE3 suggested that helices 2, 3, and 4 are flexible (*79*). This flexibility is characterized by kinks in the middle of helices 2 and 3 and occurs on the end of the four-helix bundle that contains a loop made up of residues 79−94 (the "80s loop"). The flexibility at this end of the molecule may be important for the putative opening of the four-helix bundle when associating with lipid (*79*). One may speculate that denaturation is initiated at this end of the bundle, and small differences in flexibility between the isoforms in this region may account for the differences in denaturation reported here. However, this cannot be determined precisely because the 80s loop itself is not resolved in the current X-ray structures of apoE2 and apoE4 and X-ray structures from different crystal forms are not available for these isoforms.

Monitoring denaturation by following tryptophan fluorescence is often used as an indicator of changes in tertiary structure while circular dichroism at 220 nm indicates changes in secondary structure. When a protein unfolds cooperatively, the two should follow each other identically. When the two do not coincide, this indicates the presence of folding intermediates (*71*). Guanidine-HCl denaturation monitored by fluorescence (Figure 5) shows no difference between the isoforms, but these denaturation curves are different from the denaturation curves obtained by CD measurements at a 220 nm wavelength. Recent studies of apolipophorin-III (*80*) and apoA-I (*78*) also found differences between tertiary and secondary structure denaturation of the protein. The relatively small red shift from 0 to 5 M guanidine-HCl for the 22-kDa fragment of apoE suggests at least some of the tryptophans may already be in a polar environment in the native state (Figure 5). Interestingly, the

transition in the denaturation curves of the 22-kDa fragments of apoE monitored by fluorescence was at a higher concentration of guanidine-HCl than the denaturation monitored by CD. This is likely due to the location of the tryptophans in the 22-kDa fragment of apoE (residues 20, 26, 34, and 39). Residues 26, 34, and 39 are located in helix one. Residue 20 is located near helix one in a flexible region in the amino-terminus of the protein that is unresolved in the X-ray structure. Therefore, we are only monitoring the environment of helix one. This would explain why there is no difference between the isoforms in the denaturation curves monitored by fluorescence, since the amino acid differences occur in helices three and four. It is also possible that the major red shift in the fluorescence measurements is reflective of an intermolecular interaction. However, at this protein concentration, we do not have evidence of this occurring in the analysis by CD. Also, the analyses by CD show a difference in unfolding between the isoforms and so identical intermolecular interaction is unlikely.

Studies examining the opening of the four-helix bundle when binding lipid disks indicate that helix one pairs with helix two, and helix three with helix four (*81*−*83*). It is possible that during denaturation the four-helix bundle opens up in such a manner and helices three and four denature before helices one and two. This would account for the higher midpoint of denaturation in the curves assessed by fluorescence. Using eq 4, we calculated % helix content for the 22-kDa fragments of apoE at 3 M guanidine-HCl, approximately the midpoint of transition of denaturation as monitored by fluorescence. At this guanidine-HCl concentration, the 22-kDa fragments have approximately 40% of their original helix content left.

The functions of some folding intermediates are hypothesized to involve lipid binding and bilayer penetration (*84*). The suggestion that the folding intermediate in apoE may be an opened conformation of the four-helix bundle makes lipid binding an attractive hypothesis for a biological function of this folding intermediate and is currently being investigated. There is also a growing body of literature associating protein stability and folding intermediates in diseases associated with amyloid deposition (*85*−*89*). It is possible that the presence of a partially folded intermediate in apoE4, the least stable isoform, effects amyloid formation in Alzheimer's disease; however, apoE is known to affect a variety of biological functions, including lipid metabolism and cell growth (*3*, *14*). Whether the primary influence of apoE isoforms and their differential stability on risk for AD is related to the potential effect on amyloid formation, or an independent effect on lipid transport or cellular metabolism in the brain has yet to be determined.

It is interesting to note that while apoE4 domain interaction has been demonstrated on a lipid surface (*58*), we show it does not occur in solution. One possible explanation for the difference is that the interaction between Arg-61 and Glu-255 is disrupted easily at low concentrations of a denaturant such as guanidine-HCl. However, this does not explain why the domains do not remain associated after thrombin cleavage in buffer without any denaturant (Figure 7). It has been shown that while lipid-free apoE is a tetramer in solution, it is a monomer on the surface of a lipoprotein particle (*69*, *90*). Thus, it is possible that tetramerization in the carboxyl-terminal domain prevents domain interaction. Segrest et al. hypothesized that the association of an apolipoprotein with a lipoprotein particle is determined by the length of the helices in the apolipoprotein (*91*). Specifically, long helices are best accommodated on a large lipoprotein particle where there is less curvature. On a lipid surface, Arg-61 in the 22-kDa domain of apoE4 may act to stabilize the putative long helices in the 10-kDa fragment and that results in the preferential association of apoE4 for VLDL particles, compared to apoE3.

Summary. These studies are the first to demonstrate that the 10-kDa and 22-kDa domains unfold independently of each other in apoE2 and apoE4, as do the domains in apoE3. In addition, guanidine-HCl, urea and thermal denaturation studies revealed differences among the isoforms, specifically in the unfolding of the 22-kDa domain, where the amino acid differences distinguishing the isoforms occur. ApoE4 was shown to be the least stable, and apoE2 the most stable. In addition, the guanidine-HCl denaturation studies suggested the presence of a folding intermediate in apoE, although it remains to be confirmed and further characterized. Also, both thermal and guanidine-HCl denaturations confirm that the 10-kDa fragment of apoE behaves similarly to other apolipoproteins, such as apoA-I. These studies represent the first physical characterization comparing all three common isoforms. The differences that were observed are likely, in a manner yet to be determined, to contribute to the biochemical differences and, ultimately, to the pathological consequences associated with each of the isoforms.

ACKNOWLEDGMENT

The authors thank John C. W. Carroll and Neile Shea for graphics production, Yvonne Newhouse for technical assistance, Brian Auerbach for manuscript preparation and Stephen Ordway and Gary Howard for editorial assistance.

REFERENCES

1. Rall, S. C., Jr., Weisgraber, K. H., and Mahley, R. W. (1982) *J. Biol. Chem. 257*, 4171−4178.
2. Mahley, R. W. (1988) *Science 240*, 622−630.
3. Weisgraber, K. H. (1994) *Adv. Protein Chem. 45*, 249−302.
4. Pitas, R. E., Boyles, J. K., Lee, S. H., Hui, D., and Weisgraber, K. H. (1987) *J. Biol. Chem. 262*, 14352−14360.
5. LaDu, M. J., Gilligan, S. M., Lukens, J. R., Cabana, B. G., Reardon, C. A., Van Eldik, L. J., and Holtzman, D. M. (1998) *J. Neurochem. 70*, 2070−2081.
6. Krieger, M., and Herz, J. (1994) *Annu. Rev. Biochem. 63*, 601−637.
7. Kim, D.-H., Iijima, H., Goto, K., Sakai, J., Ishii, H., Kim, H.-J., Suzuki, H., Kondo, H., Saeki, S., and Yamamoto, T. (1996) *J. Biol. Chem. 271*, 8373−8380.
8. Pitas, R. E., Innerarity, T. L., Arnold, K. S., and Mahley, R. W. (1979) *Proc. Natl. Acad. Sci. U.S.A. 76*, 2311−2315.
9. Takahashi, S., Kawarabayasi, Y., Nakai, T., Sakai, J., and Yamamoto, T. (1992) *Proc. Natl. Acad. Sci. U.S.A. 89*, 9252−9256.
10. Kounnas, M. Z., Stefansson, S., Loukinova, E., Argraves, K. M., Strickland, D. K., and Argraves, W. S. (1994) *Ann. N. Y. Acad. Sci. 737*, 114−123.
11. Avila, E. M., Holdsworth, G., Sasaki, N., Jackson, R. L., and Harmony, J. A. K. (1982) *J. Biol. Chem. 257*, 5900−5909.
12. Hui, D. Y., Harmony, J. A. K., Innerarity, T. L., and Mahley, R. W. (1980) *J. Biol. Chem. 255*, 11775−11781.
13. Boyles, J. K., Zoellner, C. D., Anderson, L. J., Kosik, L. M., Pitas, R. E., Weisgraber, K. H., Hui, D. Y., Mahley, R. W., Gebicke-Haerter, P. J., Ignatius, M. J., and Shooter, E. M. (1989) *J. Clin. Invest. 83*, 1015−1031.

14. Ishigami, M., Swertfeger, D. K., Granholm, N. A., and Hui, D. Y. (1998) *J. Biol. Chem. 273*, 20156−20161.
15. Utermann, G., Hees, M., and Steinmetz, A. (1977) *Nature 269*, 604−607.
16. Zannis, V. I., and Breslow, J. L. (1981) *Biochemistry 20*, 1033−1041.
17. Das, H. K., McPherson, J., Bruns, G. A. P., Karathanasis, S. K., and Breslow, J. L. (1985) *J. Biol. Chem. 260*, 6240−6247.
18. Weisgraber, K. H., Rall, S. C., Jr., and Mahley, R. W. (1981) *J. Biol. Chem. 256*, 9077−9083.
19. Utermann, G., Hardewig, A., and Zimmer, F. (1984) *Hum. Genet. 65*, 237−241.
20. Luc, G., Bard, J.-M., Arveiler, D., Evans, A., Cambou, J.-P., Bingham, A., Amouyel, P., Schaffer, P., Ruidavets, J.-B., Cambien, F., Fruchart, J.-C., and Ducimetiere, P. (1994) *Arterioscler. Thromb. 14*, 1412−1419.
21. Eichner, J. E., Kuller, L. H., Orchard, T. J., Grandits, G. A., McCallum, L. M., Ferrell, R. E., and Neaton, J. D. (1993) *Am. J. Cardiol. 71*, 160−165.
22. Saunders, A. M., Strittmatter, W. J., Schmechel, D., St George-Hyslop, P. H., Pericak-Vance, M. A., Joo, S. H., Rosi, B. L., Gusella, J. F., Crapper-MacLachlan, D. R., Alberts, M. J., Hulette, C., Crain, B., Goldgaber, D., and Roses, A. D. (1993) *Neurology 43*, 1467−1472.
23. Corder, E. H., Saunders, A. M., Strittmatter, W. J., Schmechel, D. E., Gaskell, P. C., Small, G. W., Roses, A. D., Haines, J. L., and Pericak-Vance, M. A. (1993) *Science 261*, 921−923.
24. Friedman, G., Froom, P., Sazbon, L., Grinblatt, I., Shochina, M., Tsenter, J., Babaey, S., Yehuda, A. B., and Groswasser, Z. (1999) *Neurology 52*, 244−248.
25. Mayeux, R., Ottman, R., Maestre, G., Ngai, C., Tang, M.-X., Ginsberg, H., Chun, M., Tycko, B., and Shelanski, M. (1995) *Neurology 45*, 555−557.
26. Nicoll, J. A. R., Roberts, G. W., and Graham, D. I. (1995) *Nat. Med. 1*, 135−137.
27. Utermann, G., Jaeschke, M., and Menzel, J. (1975) *FEBS Lett. 56*, 352−355.
28. Zannis, V. I., and Breslow, J. L. (1980) *J. Biol. Chem. 255*, 1759−1762.
29. Corder, E. H., Saunders, A. M., Risch, N. J., Strittmatter, W. J., Schmechel, D. E., Gaskell, P. C., Jr., Rimmler, J. B., Locke, P. A., Conneally, P. M., Schmader, K. E., Small, G. W., Roses, A. D., Haines, J. L., and Pericak-Vance, M. A. (1994) *Nat. Genet. 7*, 180−184.
30. Weisgraber, K. H., Innerarity, T. L., and Mahley, R. W. (1982) *J. Biol. Chem. 257*, 2518−2521.
31. Gregg, R. E., Zech, L. A., Schaefer, E. J., Stark, D., Wilson, D., and Brewer, H. B., Jr. (1986) *J. Clin. Invest. 78*, 815−821.
32. Steinmetz, A., Jakobs, C., Motzny, S., and Kaffarnik, H. (1989) *Arteriosclerosis 9*, 405−411.
33. Weisgraber, K. H. (1990) *J. Lipid Res. 31*, 1503−1511.
34. Nathan, B. P., Chang, K.-C., Bellosta, S., Brisch, E., Ge, N., Mahley, R. W., and Pitas, R. E. (1995) *J. Biol. Chem. 270*, 19791−19799.
35. Ji, Z.-S., Pitas, R. E., and Mahley, R. W. (1998) *J. Biol. Chem. 273*, 13452−13460.
36. Strittmatter, W. J., Saunders, A. M., Schmechel, D., Pericak-Vance, M., Enghild, J., Salvesen, G. S., and Roses, A. D. (1993) *Proc. Natl. Acad. Sci. U.S.A. 90*, 1977−1981.
37. Strittmatter, W. J., Weisgraber, K. H., Huang, D. Y., Dong, L.-M., Salvesen, G. S., Pericak-Vance, M., Schmechel, D., Saunders, A. M., Goldgaber, D., and Roses, A. D. (1993) *Proc. Natl. Acad. Sci. U.S.A. 90*, 8098−8102.
38. LaDu, M. J., Falduto, M. T., Manelli, A. M., Reardon, C. A., Getz, G. S., and Frail, D. E. (1994) *J. Biol. Chem. 269*, 23403−23406.
39. LaDu, M. J., Pederson, T. M., Frail, D. E., Reardon, C. A., Getz, G. S., and Falduto, M. T. (1995) *J. Biol. Chem. 270*, 9039−9042.
40. Huang, D. Y., Goedert, M., Jakes, R., Weisgraber, K. H., Garner, C. C., Saunders, A. M., Pericak-Vance, M. A., Schmechel, D. E., Roses, A. D., and Strittmatter, W. J. (1994) *Neurosci. Lett. 182*, 55−58.
41. Huang, D. Y., Weisgraber, K. H., Goedert, M., Saunders, A. M., Roses, A. D., and Strittmatter, W. J. (1995) *Neurosci. Lett. 192*, 209−212.
42. Strittmatter, W. J., Saunders, A. M., Goedert, M., Weisgraber, K. H., Dong, L.-M., Jakes, R., Huang, D. Y., Pericak-Vance, M., Schmechel, D., and Roses, A. D. (1994) *Proc. Natl. Acad. Sci. U.S.A. 91*, 11183−11186.
43. Handelmann, G. E., Boyles, J. K., Weisgraber, K. H., Mahley, R. W., and Pitas, R. E. (1992) *J. Lipid Res. 33*, 1677−1688.
44. Holtzman, D. M., Pitas, R. E., Kilbridge, J., Nathan, B., Mahley, R. W., Bu, G., and Schwartz, A. L. (1995) *Proc. Natl. Acad. Sci. U.S.A. 92*, 9480−9484.
45. Nathan, B. P., Bellosta, S., Sanan, D. A., Weisgraber, K. H., Mahley, R. W., and Pitas, R. E. (1994) *Science 264*, 850−852.
46. DeMattos, R. B., Curtiss, L. K., and Williams, D. L. (1998) *J. Biol. Chem. 273*, 4206−4212.
47. Miyata, M., and Smith, J. D. (1996) *Nat. Genet. 14*, 55−61.
48. Marques, M. A., Tolar, M., Harmony, J. A. K., and Crutcher, K. A. (1996) *Neuroreport 7*, 2529−2532.
49. Tolar, M., Marques, M. A., Harmony, J. A. K., and Crutcher, K. A. (1997) *J. Neurosci. 17*, 5678−5686.
50. Jordán, J., Galindo, M. F., Miller, R. J., Reardon, C. A., Getz, G. S., and LaDu, M. J. (1998) *J. Neurosci. 18*, 195−204.
51. Wetterau, J. R., Aggerbeck, L. P., Rall, S. C., Jr., and Weisgraber, K. H. (1988) *J. Biol. Chem. 263*, 6240−6248.
52. Aggerbeck, L. P., Wetterau, J. R., Weisgraber, K. H., Wu, C.-S. C., and Lindgren, F. T. (1988) *J. Biol. Chem. 263*, 6249−6258.
53. Wilson, C., Wardell, M. R., Weisgraber, K. H., Mahley, R. W., and Agard, D. A. (1991) *Science 252*, 1817−1822.
54. Lalazar, A., Weisgraber, K. H., Rall, S. C., Jr., Giladi, H., Innerarity, T. L., Levanon, A. Z., Boyles, J. K., Amit, B., Gorecki, M., Mahley, R. W., and Vogel, T. (1988) *J. Biol. Chem. 263*, 3542−3545.
55. Innerarity, T. L., Friedlander, E. J., Rall, S. C., Jr., Weisgraber, K. H., and Mahley, R. W. (1983) *J. Biol. Chem. 258*, 12341−12347.
56. Weisgraber, K. H., Innerarity, T. L., Harder, K. J., Mahley, R. W., Milne, R. W., Marcel, Y. L., and Sparrow, J. T. (1983) *J. Biol. Chem. 258*, 12348−12354.
57. Westerlund, J. A., and Weisgraber, K. H. (1993) *J. Biol. Chem. 268*, 15745−15750.
58. Dong, L.-M., Wilson, C., Wardell, M. R., Simmons, T., Mahley, R. W., Weisgraber, K. H., and Agard, D. A. (1994) *J. Biol. Chem. 269*, 22358−22365.
59. Bradley, W. A., Hwang, S.-L. C., Karlin, J. B., Lin, A. H. Y., Prasad, S. C., Gotto, A. M., Jr., and Gianturco, S. H. (1984) *J. Biol. Chem. 259*, 14728−14735.
60. Dong, L.-M., Parkin, S., Trakhanov, S. D., Rupp, B., Simmons, T., Arnold, K. S., Newhouse, Y. M., Innerarity, T. L., and Weisgraber, K. H. (1996) *Nat. Struct. Biol. 3*, 718−722.
61. Wilson, C., Mau, T., Weisgraber, K. H., Wardell, M. R., Mahley, R. W., and Agard, D. A. (1994) *Structure 2*, 713−718.
62. Dong, L.-M., and Weisgraber, K. H. (1996) *J. Biol. Chem. 271*, 19053−19057.
63. Morrow, J. A., Arnold, K. S., and Weisgraber, K. H. (1999) *Protein Expression Purif. 16*, 224−230.
64. Forstner, M., Peters-Libeu, C., Contreras-Forrest, E., Newhouse, Y., Knapp, M., Rupp, B., and Weisgraber, K. H. (1999) *Protein Expression Purif. 17*, 267−272.
65. Aune, K. C., and Tanford, C. (1969) *Biochemistry 11*, 4586−4590.
66. Sparks, D. L., Lund-Katz, S., and Phillips, M. C. (1992) *J. Biol. Chem. 267*, 25839−25847.
67. Pace, C. N. (1975) *Crit. Rev. Biochem. 3*, 1−43.
68. Shortle, D. (1995) *Adv. Protein Chem. 46*, 217−247.
69. Yokoyama, S., Kawai, Y., Tajima, S., and Yamamoto, A. (1985) *J. Biol. Chem. 260*, 16375−16382.
70. Palmer, T. (1981) *Understanding Enzymes*, Ellis Horwood, Chichester.
71. Shirley, B. A. (1995) *Methods Mol. Biol. 40*, 177−190.

72. Reijngoud, D.-J., and Phillips, M. C. (1982) *Biochemistry 21*, 2969−2976.
73. Reynolds, J. A. (1976) *J. Biol. Chem. 251*, 6013−6015.
74. Weinberg, R. B., and Spector, M. S. (1985) *J. Biol. Chem. 260*, 4914−4921.
75. Mantulin, W. W., Rohde, M. F., Gotto, A. M., Jr., and Pownall, H. J. (1980) *J. Biol. Chem. 255*, 8185−8191.
76. Gursky, O., and Atkinson, D. (1998) *Biochemistry 37*, 1283−1291.
77. Tall, A. R., Shipley, G. G., and Small, D. M. (1976) *J. Biol. Chem. 251*, 3749−3755.
78. Gursky, O., and Atkinson, D. (1996) *Proc. Natl. Acad. Sci. U.S.A. 93*, 2991−2995.
79. Segelke, B. W., Forstner, M., Knapp, M., Trakhanov, S. D., Parkin, S., Newhouse, Y. M., Bellamy, H. D., Weisgraber, K. H., and Rupp, B. *Protein Sci.* (in press).
80. Soulages, J. L., and Bendavid, O. J. (1998) *Biochemistry 37*, 10203−10210.
81. Raussens, V., Fisher, C. A., Goormaghtigh, E., Ryan, R. O., and Ruysschaert, J.-M. (1998) *J. Biol. Chem. 273*, 25825−25830.
82. Fisher, C. A., and Ryan, R. O. (1999) *J. Lipid Res. 40*, 93−99.
83. Lu, B., and Weisgraber, K. (1999) *Protein Sci. 8* (Suppl. 1), 133 (abstr.).
84. Fink, A. L. (1995) *Methods Mol. Biol. 40*, 343−360.
85. Kelly, J. W. (1996) *Curr. Opin. Struct. Biol. 6*, 11−17.
86. Sunde, M., and Blake, C. C. F. (1998) *Q. Rev. Biophys. 31*, 1−39.
87. Bychkova, V. E., and Ptitsyn, O. B. (1995) *FEBS Lett. 359*, 6−8.
88. Fink, A. L. (1998) *Folding Des. 3*, R9−R23.
89. Kelly, J. W. (1997) *Structure 5*, 595−600.
90. Funahashi, T., Yokoyama, S., and Yamamoto, A. (1989) *J. Biochem. 105*, 582−587.
91. Segrest, J. P., Garber, D. W., Brouillette, C. G., Harvey, S. C., and Anantharamaiah, G. M. (1994) *Adv. Protein Chem. 45*, 303−369.

BI000099M